THE JOURNAL OF PHYSICAL CHEMISTRY B

ARTICLE

pubs.acs.org/JPCB

Decelerated Water Dynamics and Vibrational Couplings of Hydrated DNA Mapped by Two-Dimensional Infrared Spectroscopy

Ming Yang, Łukasz Szyc, and Thomas Elsaesser*

Max-Born-Institut für Nichtlineare Optik und Kurzzeitspektroskopie, Max-Born-Strasse 2 A, D-12489 Berlin, Germany

Supporting Information

ABSTRACT: Double-stranded DNA oligomers containing 23 alternating adenine-thymine base pairs are studied at different hydration levels by femtosecond two-dimensional (2D) infrared spectrosopy. Coupled NH stretching modes of the A-T pairs and OH stretching excitations of the water shell are discerned in the 2D spectra. Limited changes of NH stretching frequencies and line shapes with increasing hydration suggest spectral dynamics governed by DNA rather than water fluctuations. In contrast, OH stretching excitations of the water shell around fully hydrated DNA undergo spectral diffusion on a ~500 fs time scale. The center line slopes of the 2D spectra of hydrated DNA demonstrate a slower decay of the frequency−time correlation function (TCF) than that in neat water, as is evident from a comparison with 2D spectra of neat H_2O and theoretical TCFs. We attribute this behavior to reduced structural fluctuations of the water shell and a reduced rate of resonant OH stretching energy transfer.

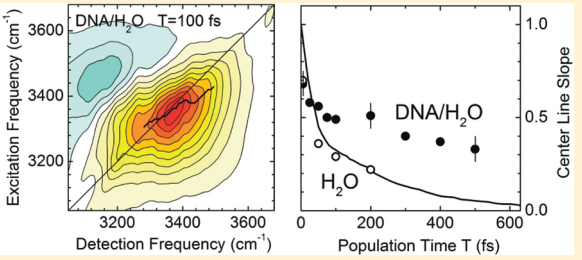

1. INTRODUCTION

The aqueous environment of biomolecules plays a key role for their equilibrium structure, structural stability, and biochemical function. The highly specific interactions at the interface between the biomolecule and the water shell are of particular relevance for such properties. The surface of deoxyribonucleic acid (DNA), a double-stranded helix structure, is characterized by the major and the minor groove of different widths and depths.[1,2] At the DNA surface, structural units such as ionic phosphate groups and sugar rings of the backbone as well as pairs of nucleic bases offer a variety of interaction sites with water molecules of the environment. As a result, the structure of the first water layer around DNA is highly heterogeneous and markedly different from bulk water. In contrast, outer water layers are expected to behave similar to bulk water. The predominant type of local interaction in the first layer is hydrogen bonding between water molecules and DNA groups and/or among water molecules. In addition, there are long-range Coulomb forces that originate from (partially) charged groups of the DNA structure, the counterions of DNA, and the water dipoles. At ambient temperature, the water shell undergoes rapid structural fluctuations that lead to fluctuating electric interactions between the charges and dipoles in the system.[3−5]

The structure of the water shell around DNA, water−DNA interactions at the molecular level, and the role of water for DNA function have been subjects of research since the discovery of the double-helix geometry. X-ray diffraction,[6−11] neutron scattering,[12] and infrared spectroscopy under stationary conditions[13−15] have provided specific information on time-averaged hydration geometries and interaction strengths. The dynamics of DNA−water interactions and related changes and fluctuations of hydration geometries in a (sub)nanosecond time range have been addressed by different techniques of nuclear magnetic resonance (NMR).[16−19]

The geometries and dynamics of DNA hydration have been studied in classical molecular dynamics (MD) simulations.[20−24] Hydration patterns averaged over a time interval on the order of 10 ns reproduce major features of hydration patterns derived from X-ray diffraction data.[21,22] Simulations of hydrogen bond dynamics at the DNA/water interface have given average hydrogen bond lifetimes on the order of 10 ps and maximum residence times between ~30 ps and several hundreds of picoseconds.[23] A MD analysis of correlation functions of hydrogen bond lifetimes between water and DNA gives multiexponential decays with time constants between 0.5 and ~200 ps. Hydrogen bonds in the minor groove are longer-lived than those in the major groove, and both persist longer than water−phosphate hydrogen bonds.[24]

Ultrafast spectroscopy provides direct access to dynamics of hydrated DNA on the femtosecond time scale of molecular motions and structural fluctuations. A first group of experiments has mapped solvation dynamics of an electronic dipole excitation of a chromphore attached to or incorporated into a DNA structure. The time-dependent Stokes shift of fluorescence from the chromophores has been measured with up to femtosecond time resolution.[25,26] In a linear response approximation, two-point frequency−time correlation functions (TCFs) have been derived from the transient Stokes shift and compared to results for chromophores in bulk water. In general, the TCFs of the DNA/chromophore systems display a slower decay, which, in

Received: August 24, 2011
Revised: September 30, 2011
Published: October 05, 2011

some cases, extends into the nanosecond time domain. This time behavior reflects structural dynamics of both the DNA structure and the water shell, which are induced by the change of the electronic dipole and spatially averaged over charged DNA groups, counterions, and many water molecules. As a result, an unambiguous extraction of the water response from such data is difficult. Nevertheless, such data have been interpreted in terms of a slowing-down of water reorientation dynamics at the surface of DNA and other proteins,[25,27] a view that has been challenged by recent ^{17}O NMR relaxation studies of proteins[28] and molecular dynamics simulations.[29] A second issue is the structurally invasive character of the fluorescence probes, which leads to changes of both the DNA and hydration geometries.[30]

A second class of experiments makes use of femtosecond vibrational spectroscopy, in particular, two-dimensional (2D) nonlinear infrared spectroscopy,[31−37] in which vibrational excitations serve as probes of molecular interactions and dynamics in the electronic ground state. Selecting particular vibrations of DNA or water, molecular couplings and ultrafast processes in the macromolecular structure and the hydration shell can be separated. So far, femtosecond pump−probe experiments and 2D infrared spectroscopy of DNA have concentrated on base pair vibrations, that is, modes in the fingerprint range and NH stretching modes.[36−40] Recently, the subpicosecond lifetimes and the vibrational couplings of NH stretching modes in artificial DNA oligomers have been studied by 2D spectroscopy at a very low hydration level.[37] The interaction of phosphate groups in the DNA backbone with their water shell has been mapped in femtosecond pump−probe experiments in which the asymmetric $(PO_2)^-$ vibration was chosen as a local probe.[40] The water shell serves as an efficient sink of vibrational excess energy with subpicosecond energy-transfer times from the phosphate group to the water environment.

In this article, we report the first study of the dynamics of DNA hydration by femtosecond 2D infrared spectroscopy. We study artificial double-stranded DNA oligomers containing 23 alternating adenine-thymine (A-T) base pairs in Watson−Crick geometry.[37−40] Both NH stretching oscillators of the A-T base pairs and OH stretching oscillators in the water shell serve as direct probes of hydration dynamics. We present a series of 2D measurements in a wide range of hydration levels, allowing for a clear separation of NH stretching excitations of A-T pairs and OH stretching vibrations of water. The NH stretching modes display a mutual coupling and vibrational energy transfer similar to their behavior at very low water content.[37] Their line shapes display limited changes with water concentration, even under conditions of full DNA hydration. In contrast, OH stretching excitations undergo pronounced spectral diffusion on a time scale distinctly longer than that in bulk water. Processes of energy redistribution are clearly resolved in the transient 2D spectra.

2. EXPERIMENTAL METHODS

We study artificial double-stranded DNA oligomers containing 23 alternating (A-T) base pairs (Figure 1a) in Watson−Crick geometry (inset of Figure 1b; supplier Thermo Scientific, HPLC, desalted). To generate thin films of high optical quality, the sodium counterions of the oligomers were replaced by cetyltrimethyl-ammonium chloride (CTMA), a surfactant forming complexes with DNA.[38,41,42] The ∼10 μm thick films were cast on 500 nm thick Si_3N_4 substrates. There was no contribution of the substrates to the nonlinear optical signal. The DNA concentration in

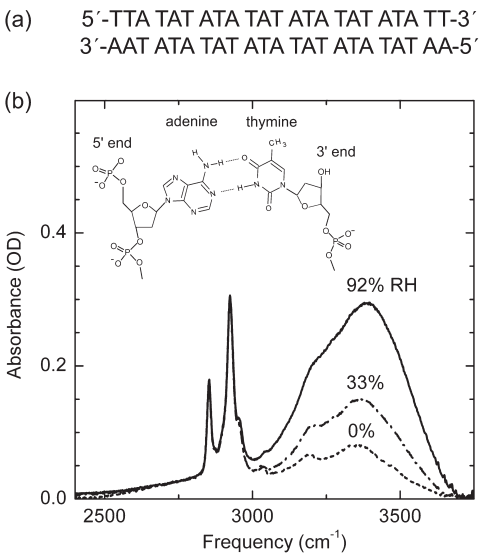

Figure 1. (a) Sequence of alternating adenine-thymine (A-T) base pairs in the double-stranded DNA oligomers. (b) Linear infrared absorption spectrum of a DNA thin film sample at 0, 33, and 92% RH (lines). The spectrum between 2500 and 4000 cm^{-1} consists of the CH stretch components below 3000 cm^{-1}; that between 3000 and 3700 cm^{-1} consists of the NH and NH_2 stretching absorption and, at the higher hydration levels, the OH stretching absorption of water. Inset: Molecular structure of the A-T base pair in Watson−Crick geometry and the sugar and phosphate groups of the DNA backbone.

the films was approximately 1.5×10^{-2} M. The film samples were integrated into a home-built humidity cell that was connected to a reservoir. By putting various agents into the reservoir, we controlled the relative humidity (RH) in the cell and the film sample.[14,15] RH values of 0 (agent P_2O_5), 33 ($MgCl_2$), and 92% ($NaBrO_3$) correspond to a water concentration of 2, 6, and more than 20 water molecules per base pair. For 92% RH, the DNA oligomers are fully hydrated, as was confirmed independently by measuring the frequency position of the asymmetric $(PO_2)^-$ stretching band, a sensitive probe of the hydration level.[14,15]

In general, the conformation of DNA helices depends on the hydration level.[1] X-ray diffraction has shown that DNA helices with alternating A-T base pairs exist in B-like conformations at a humidity level higher than approximately 70% RH.[43,44] Theoretical calculations[45] and infrared spectroscopy[46,47] have suggested that DNA containing A-T base pairs displays a B-helix for a wide humidity range and rarely undergoes conformational transitions. The frequency positions of phosphodiester backbone vibrations coupled to the sugar motions and the glycosidic bond torsion are sensitive probes of DNA conformation. In our samples, two infrared bands at 835 and 890 cm^{-1}, which are characteristic for the B-geometry,[46,47] are observed at 92% RH. Upon reducing the water content to 33% RH, these bands undergo minor shifts of 2−3 cm^{-1}, that is, the B-form prevails. In the whole range from 0 to 92% RH, infrared bands characteristic for the A-form of DNA at 805 and 860 cm^{-1} are absent.

The 2D spectra are derived from heterodyne-detected three-pulse photon echoes.[32,34,35,48] A parametric infrared source driven by a regeneratively amplified Ti:sapphire laser system (repetition rate of 1 kHz) provides pulses of up to 7 μJ energy tunable from 2800 to 4000 cm^{-1} (spectral pulse width > 250 cm^{-1}). The pulses were characterized by frequency-resolved optical gating (FROG), giving a Gaussian temporal envelope, a

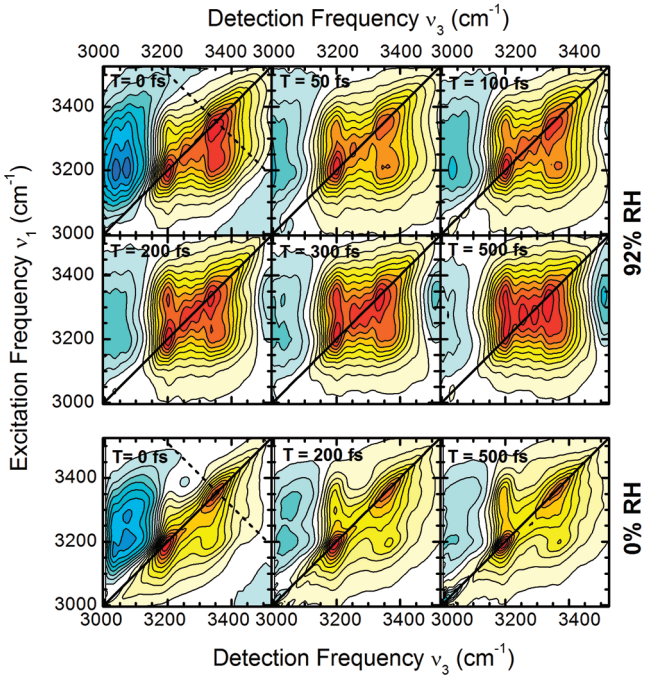

Figure 2. Absorptive 2D spectra of DNA oligomers at 92 (upper two rows) and 0% RH (lower row, ref 37) measured in the (∥⊥⊥) polarization configuration. The 2D signals are corrected for the spectra of the third and the local oscillator pulse in the photon-echo measurements. The positive signals (yellow−red part) are due to the $\nu = 0$ to 1 transitions of NH and OH stretching oscillators, and the negative signals at small ν_3 (green−blue part) are due to the $\nu = 1$ to 2 transitions. Negative signals at large ν_3 in the 92% RH spectra are due to the hot water ground state. Each spectrum is normalized to the respective maximum positive signal with contour lines corresponding to 10% changes in amplitude. Dashed lines in the $T = 0$ fs panels: Antidiagonal along which the cuts in Figure 3c,d were generated.

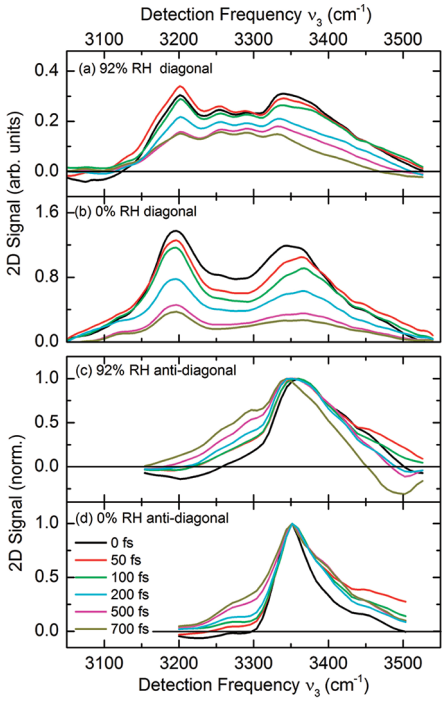

Figure 3. Cross sections through the 2D spectra recorded at 92 (Figure 2) and 0% RH (Figure 2 and ref 37) at different population times T. (a,b) Cross sections along the diagonal $\nu_1 = \nu_3$. (c,d) Cross sections along the antidiagonal crossing the diagonal at (3350,3350) cm^{-1} (dashed lines in the $T = 0$ fs panels of Figure 2).

pulse duration between 50 and 70 fs, and a time−bandwidth product of ∼0.5. Two phase-locked pulse pairs are generated with diffractive optics.[49] They serve for generating photon echo signals as a function of the coherence time τ, the delay between pulses 1 and 2, and the population time T, the delay between pulses 2 and 3 interacting with the DNA sample. The resulting photon echo signal is heterodyned with pulse 4, the local oscillator, and detected by spectral interferometry. Details of the photon echo setup and the procedures applied for data analysis have been presented in refs 34 and 48. 2D spectra measured with the same DNA oligomers at 0% RH have been reported in ref 37.

The 2D spectra presented here were measured with pulses centered at 3250 (Figures 2 and S1 (Supporting Information)) and 3400 cm^{-1} (Figure 5). We applied two different polarizations scheme with (i) parallel linear polarizations of all 4 pulses (∥∥∥) and (ii) parallel linear polarizations of pulses 1 and 2 and perpendicular linear polarizations of pulses 3 and 4 (∥⊥⊥). Here, we focus on spectra measured with the (∥⊥⊥) scheme. In all measurements, the fraction of excited NH and OH stretching oscillators was less than 1%.

3. RESULTS

Linear infrared absorption spectra of the DNA films between 2500 and 3800 cm^{-1} are shown in Figure 1b for 0, 33, and 92% RH. The strong narrow bands below 3000 cm^{-1} are due to the different CH stretching modes of the DNA oligomers and the CTMA counterions. The spectrally broad absorption between 3000 and 3700 cm^{-1} represents the NH and NH_2 stretching bands of the A-T base pairs and the OH stretching band of water. At 0% RH, the overall absorption is dominated by the different NH stretching bands with a minor contribution of water.[38,39] With increasing water concentration, the OH stretching absorption becomes more pronounced and dominates at 92% RH. Because of the smooth unstructured line shapes at higher RH, a decomposition of the linear spectra into the different underlying NH and OH stretching components is not possible.

Absorptive 2D correlation spectra of DNA films at 0, 33, and 92% RH were derived from heterodyne-detected photon echoes. In the following, we focus on 2D spectra recorded at 92% RH, that is, with fully hydrated DNA oligomers, and compare them to our previous measurements at 0% RH.[37] Data recorded at 33% RH, that is, with partially hydrated DNA, are presented in the Supporting Information. In Figure 2, we show 2D spectra of DNA at 92% RH for six different population times T (upper two rows) and of DNA at 0% RH for three different values of T (bottom row). In each panel, the sum of the rephasing and nonrephasing 2D signal[50] is plotted as a function of the excitation frequency ν_1 (ordinate) and the detection frequency ν_3 (abscissa) for the (∥⊥⊥) polarization configuration. The 2D spectra were corrected for spectral pulse envelopes by dividing the 2D signals by the electric field spectra of the third interacting pulse ($\mathbf{k}_3$) and the local oscillator pulse. The 2D spectra display negative signals (blue contours) at low detection frequencies ν_3, which originate from $\nu = 1$ to 2 transitions of excited oscillators. The positive signals at higher ν_3 are due to the $\nu = 0$−1 transitions

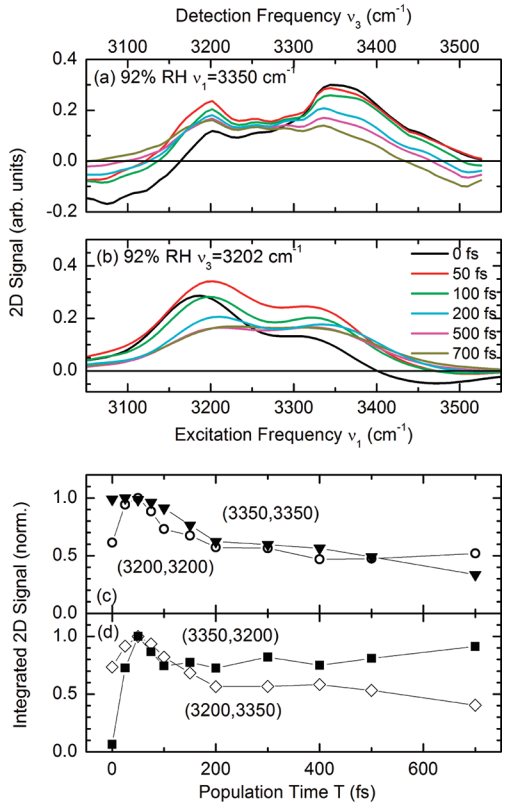

Figure 4. Cross sections through the 2D spectra recorded at 92% RH at different population times T (cf. Figure 2). (a) Cross sections along the detection frequency axis for an excitation frequency of ν_1 = 3350 cm^{-1}. (b) Cross section along the excitation frequency axis for a detection frequency of ν_3 = 3202 cm^{-1}. (c,d) Spectrally integrated intensity of the 2D signals recorded at 92% RH as a function of population time for the peaks (ν_1,ν_3) = (3200,3200), (3350,3350), (3350,3200), and (3200,3350) cm^{-1}.

(yellow−red contours). For ν_3 > 3450 cm^{-1}, the spectra for 92% RH exhibit a negative signal due to the delayed buildup of a vibrationally hot ground state of the water shell, which will be discussed in the Supporting Information.

There is a common pattern of spectral peaks at *all* hydration levels, consisting of two pronounced maxima at 3200 and 3350 cm^{-1} on the diagonal ν_1 = ν_3 and cross peaks at (ν_1,ν_3) = (3350,3200) and (3200,3350) cm^{-1}. The 92% RH spectra display a second contribution of similar strength underneath and in between such peaks that undergoes a pronounced reshaping as a function of population time T. For a more detailed inspection and comparison, we plot spectral cross sections along the diagonal ν_1 = ν_3 in Figure 3a (92% RH) and b (0% RH), as well as cross sections along an antidiagonal (dashed lines in the T = 0 fs panels of Figure 2 crossing the (ν_1,ν_3) = (3350,3350) cm^{-1} position in Figure 3c (92% RH) and d (0% RH). While the diagonal cuts for 0% RH (Figure 3b) display distinct maxima at 3200 and 3350 cm^{-1} and a minor reshaping for all population times T, the data for 92% RH (Figure 3a) exhibit additional signal in between the two peaks that reaches, with increasing T, an amplitude similar to that of the peaks. Furthermore, the negative signal caused by the buildup of the hot water ground state (cf. Figure 2) results in a reshaping of the spectral cuts at detection frequencies ν_3 > 3400 cm^{-1} that is absent at 0% RH.

The antidiagonal cross sections for 0% RH (Figure 3d) show the peak at 3350 cm^{-1} (located on the diagonal) with a sharp

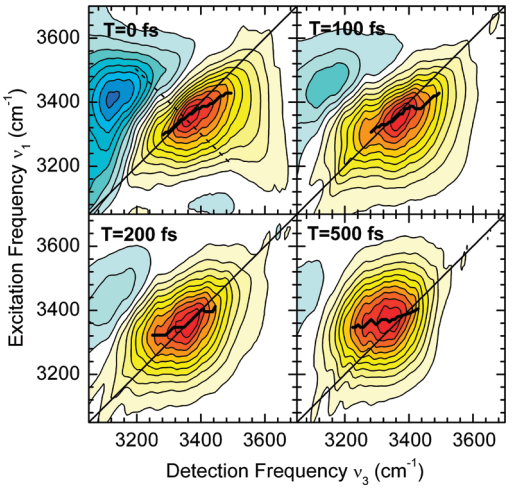

Figure 5. 2D spectra of hydrated DNA at 92% RH measured with femtosecond pulses centered at 3400 cm^{-1} (∥⊥⊥ polarization scheme). In contrast to Figures 2 and S1 (Supporting Information), the spectra are corrected for the local oscillator spectrum only (as spectra in ref 41.). Thick solid lines: Center lines derived from cross sections along the excitation frequency axis ν_1. Dashed line in the T = 0 fs panel: Antidiagonal direction along which the cuts in Figure 6a were taken.

edge at low detection frequencies and a comparably weak (off-diagonal) shoulder growing in over a period of 700 fs. At 92% RH (Figure 3c), one finds a spectrally wider and stronger shoulder that builds up on a similar time scale. The overall reshaping of the broad component found at 92% RH leads to essentially round contours in the outer parts of the T = 500 fs 2D spectrum (Figure 2).

All spectra in Figure 2 and Figure S1 (Supporting Information) display cross peaks at (ν_1,ν_3) = (3350,3200) and (3200,3350) cm^{-1}, positions which remain unchanged for all population times T. The relative intensity of the cross peak at (3350,3200) cm^{-1} increases with T, as is evident from the cross sections of the 92% RH spectra along the detection frequency in Figure 4a and along the excitation frequency in Figure 4b. A similar rise hase been observed at 0% RH.[37] In Figure 4, we present spectrally integrated 2D signals derived from the 92% RH spectra for (c) the diagonal peaks at (3200,3200) cm^{-1} and (3350, 3350) cm^{-1} and (d) the cross peaks at (3350, 3200) cm^{-1} and (3200,3350) cm^{-1}. All peaks show a partial initial decay followed by a slower subpicosecond time evolution. Such kinetics are in agreement with the time constants of ν = 1 relaxation of the oscillators of ∼500 fs and subsequent energy redistribution as observed in femtosecond pump−probe experiments.[39] In contrast to all other peaks, the intensity of the cross peak at (3350,3200) cm^{-1} increases slightly with increasing T.

The 2D spectra recorded at a hydration level of 33% RH (Figure S1, Supporting Information) display both the peak pattern and the broad "background" contribution, the latter, however, with a smaller relative strength than that at 92% RH. Changes in the spectral cuts, which are shown in Figure S2 (Supporting Information), occur in a time range similar to the 0 and 92% RH data.

To facilitate a direct comparison of water dynamics around DNA with neat water, we recorded 2D spectra of DNA at 92% RH with femtosecond pulses centered at 3400 cm^{-1}. The 2D spectra of neat water reported in ref 48 were measured under similar experimental conditions. In Figure 5, we show 2D spectra of DNA at 92% RH, plotted with a correction for the local

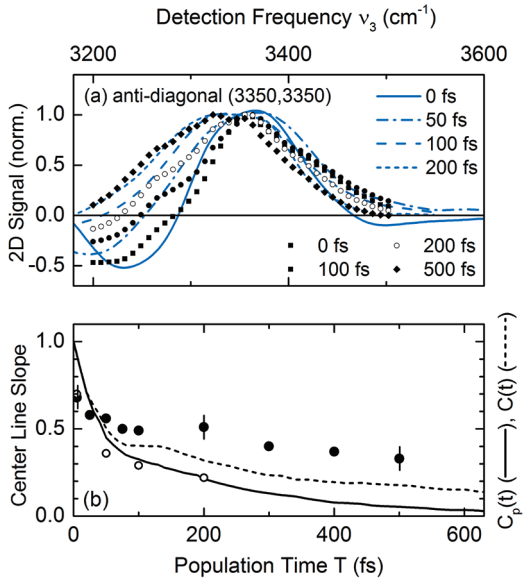

Figure 6. (a) Antidiagonal cuts of the 2D spectra of neat water (blue lines, derived from data in ref 48, temperature 304 K) and of the 2D spectra of DNA at 92% RH (symbols, cut along dashed line in Figure 5). Spectral diffusion of the DNA water shell is slower than that of bulk water. (b) Slope of the center lines of 2D spectra of Figure 5 as derived from a linear fit of the center slope lines (solid symbols). The open symbols represent the center line slopes derived from 2D spectra of neat water (ref 48) and display a faster initial correlation decay. Lines: TCFs of bulk water calculated from molecular dynamics simulations (ref 56) with ($C_p(t)$) and without ($C(t)$) resonant energy transfer between OH stretching oscillators.

oscillator spectrum only (as in Figure 1 of ref 48). The 2D spectra are dominated by OH stretching excitations of the water shell and exhibit a transition from a diagonal to an essentially round line shape, that is, spectral diffusion, on a time scale of 500 fs. The thick solid lines in Figure 5 represent the center lines of the 2D spectra as derived from cross sections along the excitation frequency axis ν_1.[51] In Figure 6a, we compare normalized spectral cross sections (symbols) along the antidiagonal in Figure 5 (dashed line in the T = 0 fs panel) with results for neat water (blue lines, derived from the 2D spectra in ref 48; sample temperature of 304 K). The antidiagonal cuts of both the DNA and water 2D spectra exhibit the formation of a strong shoulder at low detection frequencies. In the DNA hydration shell, this spectral evolution is slowed down compared to neat water.

4. DISCUSSION

The 2D spectra give insight into both NH stretching excitations of the A-T base pairs and OH stretching excitations of water molecules. The spectra are characterized by broad line shapes with a substantial overlap of the different diagonal and off-diagonal components. In the following section 4.1, we address the vibrational assignments of the different peaks to discern NH and OH stretching contributions. This is followed by a discussion of the NH stretching line shapes. In section 4.2, the dynamics of OH stretching excitations and the underlying structural dynamics of the water shell are discussed.

4.1. Vibrational Assignments and NH Stretching Line Shapes. The 2D spectra recorded with pulses centered at 3250 cm^{-1} (Figure 2, Figure S1 (Supporting Information)) display the same pattern of positive diagonal and cross peaks at *all* hydration levels, that is, the spectral positions of the peaks remain unchanged upon increasing hydration. At 0% RH, corresponding to a residual water concentration of two water molecules per base pair, NH stretching excitations of the A-T base pairs strongly dominate the 2D spectra. We, thus, assign the peak pattern to the different NH stretching excitations of adenine and thymine.[37] The diagonal peak at 3350 cm^{-1} is attributed to the asymmetric NH_2 stretching vibration of adenine, while the diagonal peak with maximum at 3200 cm^{-1} consists of two components arising from the NH stretching mode of thymine and the symmetric NH_2 stretching mode of adenine. The cross peaks at (ν_1,ν_3) = (3200,3350) cm^{-1} and (3200,3350) cm^{-1} demonstrate a coupling between the NH stretching oscillators. At 0% RH, the relative intensity of the cross peak at (3350,3200) cm^{-1} increases as a function of population time T (cf. Figure 2) due to a downhill vibrational energy transfer from the asymmetric NH_2 stretching vibration of adenine to the NH stretching oscillator of thymine.[37] In the antidiagonal spectral cuts for 0% RH (Figure 3d), the enhancement of this cross peak is reflected in the T-dependent rise of the weak off-diagonal shoulder at around 3270 cm^{-1}. From the subpicosecond kinetics of the intensity rise, a vibrational coupling on the order of 5 cm^{-1} has been derived.[37] The data summarized in Figures 4 (92% RH) and S2 (Supporting Information) (33% RH) show clearly that a similar downhill energy transfer occurs at the higher hydration levels.

At 33 and 92% RH, the NH stretching peaks are complemented by a spectrally broad contribution that originates from OH stretching excitations of the water shell. At 92% RH, the amplitudes of NH and OH stretching components are similar. With increasing population time T, the OH stretching line shape undergoes a reshaping toward a circular envelope caused by spectral diffusion of the OH excitations. This reshaping is manifested in the rise of relative intensity in between the diagonal peaks at 3200 and 3350 cm^{-1} (Figure 3a) and contributes to the time-dependent enhancement of the strong shoulder between 3200 and 3300 cm^{-1} in the antidiagonal cuts of Figure 3c. It should be recalled that the intensity growth of the NH stretch cross peak at (3350,3200) cm^{-1} also contributes to this shoulder. A comparison of the 2D spectra for 92 (Figures 2 and 3) and 33% RH (Figures S1 and S2, Supporting Information) demonstrates that the amplitude of the OH stretch component relative to the NH stretch peak pattern is substantially higher at 92% RH. We conclude that (i) the NH and OH stretching contributions are essentially additive and (ii) the line shapes of the NH stretching peaks are rather insensitive to an increasing level of hydration, that is, there is a moderate spectral broadening around unchanged spectral positions only.

In the 2D spectra, the diagonal and off-diagonal NH stretching peaks overlap in part with each other and with the time-dependent OH stretching envelope, making a quantitative line shape analysis very difficult. In particular, nodal and/or center lines[31,51] in such congested 2D spectra have a highly complex shape that does not allow for a clear separation of the different components and their spectral dynamics. Nevertheless, the shape and the spectral widths of the diagonal peaks give insight into the broadening mechanisms and the overall time scale of vibrational dephasing of NH stretching excitations. To compare the line broadenings due to vibrational dephasing at the different hydration levels, we consider the spectral width $\Delta\nu_a$ (fwhm) of the NH stretching diagonal peaks along the antidiagonals crossing at (ν_1,ν_3) = (3200,3200) and (3350,3350) cm^{-1}. At 0 and 33% RH, the diagonal peaks at (3200,3200) and (3350,3350) cm^{-1} display a respective $\Delta\nu_a$ = 70 and 90 cm^{-1}, both remaining unchanged with

increasing population time T. At 92% RH, the diagonal peaks at (3200,3200) and (3350,3350) cm^{-1} show values of $\Delta\nu_a \approx 90\ cm^{-1}$ and $\Delta\nu_a = 125\ cm^{-1}$. Such absolute values of $\Delta\nu_a$ clearly point to a decay component in the TCF on a time scale of a few hundreds of femtoseconds.

The NH stretching oscillators are subject to fluctuating long-range Coulomb forces exerted by the ionic phosphate groups in the DNA backbone, the counterions, and the water molecules in the hydration shell, resulting in vibrational dephasing. The moderate changes of the 2D line shapes and $\Delta\nu_a$ of NH stretching excitations when going from 0 to 92% RH suggest that fluctuating forces originating from the DNA structure itself play a prominent role in their vibrational dephasing. The frequency spectrum of the fluctuating force is governed by vibrational motions of the helix structure and the counterions, while translational and rotational motions are much too slow to account for subpicosecond dephasing. Both experiment and theory have shown that delocalized vibrations of the backbone and motions of the counterions relative to the DNA helix occur in the frequency range from ~1 up to 200 cm^{-1}.[52−54] Such modes involve large-amplitude elongations of the charged counterions and phosphate groups and, thus, should dominate the low-frequency spectrum of the fluctuating Coulomb forces. The different bending and stretching motions of the phosphate ions are of smaller amplitude and occur between approximately 400 and 1300 cm^{-1}, complemented by a large number of fingerprint modes of the sugar groups and base pairs extending up to frequencies of approximately 1750 cm^{-1}.[55] At room temperature (thermal energy $kT = 200\ cm^{-1}$), thermally excited modes below 600 cm^{-1} dominate the fluctuating Coulomb forces and give rise to the fast dephasing of the NH stretching excitations. A thorough analysis of dephasing by DNA motions requires theoretical calculations of the vibrational force fields in combination with molecular dynamics simulations of the microscopic motions.

It is interesting to consider the limited role of water fluctuations in NH stretch dephasing from the viewpoint of the molecular structure of hydrated DNA. At 0 and 33% RH, water molecules are predominantly located at the phosphate groups in the DNA backbone and at the counterions nearby, while base pair hydration is imcomplete. For full hydration at 92% RH, both the minor and the major grooves of the double helix (in the B-form) are hydrated, and local interactions between water molecules and NH groups of the bases become possible. However, the strongest local interaction of the NH group of thymine (cf. Figure 1b) is the hydrogen bond to the N1 atom of adenine, a structural feature that is not affected by the water shell and remains unchanged on the time scale of the 2D experiments. The NH_2 group of adenine is part of the second hydrogen bond within the A-T base pair but offers a free NH unit that is accessible for forming an intermolecular hydrogen bond with a water molecule in the major groove of the double helix. X-ray diffraction data suggest that hydrogen bonds at this position are weak (N···O distance of the order of 0.35 nm) as water molecules interact more strongly with the neighboring N7 position of the adenine structure.[7,8] Moreover, MD simulations indicate that (i) the reorientation dynamics of water molecules in the major grooves occur in the picosecond time domain with a 1.4 ps component representing the fastest decay component of the dipole−dipole time correlation function and (ii) the majority of water−DNA hydrogen bonds in the major groove have picosecond lifetimes.[24] This suggests that fluctuations of the local water structure around the NH_2 groups are too slow to contribute to the subpicosecond spectral diffusion of NH stretching excitations.

4.2. Vibrational and Structural Dynamics of the Water Shell. We now address the dynamics of OH stretching excitations of the water shell, while the formation of a vibrationally hot ground state by energy disspation is discussed in the Supporting Information. While spectral diffusion of the OH stretching component is clearly present in the 2D spectra of Figures 2 and S1 (Supporting Information), an analysis is hampered by the overlapping pattern of NH stretching peaks of similar strength. In contrast, the 2D spectra recorded with pulses centered at 3400 cm^{-1} (Figure 5) are strongly dominated by OH stretching excitations and, thus, give specific insight into spectral diffusion in the hydration shell around DNA. As a reference, we use the 2D spectra of neat H_2O measured at a temperature of 304 K (Figure 1 of ref 48). As a function of population time T, one observes a reshaping from an initially elliptic spectral envelope along the diagonal to an essentially round envelope at late T in both hydrated DNA and neat water. This behavior gives direct evidence of spectral diffusion that randomizes the OH stretching frequencies. In the case of hydrated DNA, spectral diffusion extends over the T interval of 500 fs studied here and most probably continues on a longer time scale. In contrast, spectral diffusion of OH stretching excitations in neat water occurs to a major extent within the first 100−200 fs after excitation.[34,48] The slowing down of spectral diffusion in the hydration shell of DNA is evident when comparing spectral cross sections of the two sets of spectra (Figure 6a). The cross sections along the antidiagonal going through $(\nu_1,\nu_3) = (3350,3350)\ cm^{-1}$ exhibit a strong T-dependent broadening toward lower detection frequencies, a hallmark of the spectral diffusion of OH stretching excitations. In neat water, the antidiagonal width increases strongly within the first 100 fs and reaches its final value after 200 fs when the envelope of the corresponding 2D spectrum is round. In contrast, the water shell of DNA displays spectral dynamics slowed down by at least a factor of 2 to 3.

For a more detailed analysis, we consider the slope of the center lines of the 2D spectra of DNA/water (thick solid lines in Figure 5) and compare it to results for neat water. The change in slope with increasing population time T is related to the TCF of the fluctuating ensemble.[51] In Figure 6b, we plot the center line slope, derived from a linear fit of the center lines in Figure 5, as a function of T for the full set of DNA 2D spectra recorded with excitation at 3400 cm^{-1} (solid symbols). Center line slopes derived from the 2D spectra of neat water in ref 48 are shown as open symbols. While the value of the slope at $T = 0$ is similar in the two cases, the data for neat water exhibit a much faster decay within the first 50 to 100 fs, which has been attributed to spectral diffusion caused by librational motions and, in part, to resonant energy transfer between OH stretching oscillators.[34,48] This component is (if it exists at all) much weaker in the DNA/water data, which are dominated by a gradual and incomplete decay of correlation extending over a period of 500 fs.

For comparison, Figure 6b shows TCFs of OH stretching excitations of bulk water as calculated from molecular dynamics simulations.[56] The solid line ($C_p(t)$) is the result of a calculation including resonant energy transfer between OH stretching oscillators, while the dashed line ($C(t)$) neglects this process. The comparison of the DNA/water results (solid symbols) with the calculated correlation functions shows that (i) the amplitude of the fast sub-100 fs component is strongly reduced in the DNA/water system and (ii) the subsequent time evolution of

DNA/water between T = 100 and 500 fs is closer to $C(t)$ than to $C_p(t)$. In particular, the DNA/water data do not show the pronounced decay of $C_p(t)$ between 70 and 600 fs.

The structure of the water shell around DNA with a highly heterogeneous first layer of water molecules and more bulk-like geometries in the outer parts is quite different from that of bulk water. The overall water concentration in our thin-film samples is on the order of 10 M compared to 56 M in bulk water. At such reduced concentration, resonant energy transfer between OH stretching oscillators[56−58] is slowed down substantially. Extrapolating from an experimental study of resonant energy transfer between diluted OH stretching oscillators (HOD in D_2O, ref 58), one estimates picosecond energy-transfer times within the water shell that are longer than the subpicosecond vibrational lifetime of the OH stretching oscillators. A substantial fraction of the water molecules (approximately 20 water molecules per base pair including the backbone phosphate and sugar units) is located in the first hydration layer that is attached to particular DNA sites by hydrogen bonds. Such local interactions slow down or even suppress orientational and translational water motions. For instance, motions of water molecules in the narrow minor groove of the helix are sterically hindered, and hydrogen bond lifetimes are much longer than those in bulk water, as found in NMR measurements and MD simulations of correlation functions of hydrogen bond lifetimes. The partial suppression of low-frequency water motions and the longer hydrogen bond lifetimes directly affect the frequency spectrum of the fluctuating Coulomb forces and result in a slowing down of the different decay components in the TCF of the OH stretching excitations.

The slowing down of spectral diffusion derived from our experiments compares favorably with theoretical simulations of water dynamics at DNA surfaces.[29] Such analysis of polar solvation of electronic dipole excitations gives decay times of the water frequency fluctuation correlation function of 0.4 and 2.7 ps in the electronic ground state and suggests solvation to be dominated by the water molecules in the first hydration shell. However, the incorporation of a chromophore into DNA modifies the initial DNA structure, the local hydrogen bond pattern, and interactions substantially. A recent theoretical simulation has given insight into such effects for a hydrated DNA dodecamer.[30] It shows that the replacement of an A-T pair by a coumarin chromophore results in a widening of the minor groove, an increased mobility of water molecules, and a shortening of rotational reorientation times. Further theoretical calculations and simulations are required for an in-depth comparison with our experimental results.

5. CONCLUSIONS

In conclusion, we have studied the interaction of DNA with its hydration shell by mapping ultrafast vibrational dynamics in the electronic ground state of oligomers containing 23 alternating A-T base pairs. Two-dimensional infrared spectra for a wide range of hydration levels allow for a clear separation of the response of NH stetching vibrations of DNA from the ultrafast dynamics of OH stretching excitations of the water shell. The spectral positions and line shapes of NH stretching excitations are not modified much with increasing hydration, the main change being an increase of the antidiagonal line width by approximately 25%. This result suggests that the NH stretching excitations are essentially localized to the particular base pair that undergoes minor geometry changes upon hydration. Moreover, it points to a limited influence of water fluctuations on such modes, a behavior that is in line with the comparably slow structural dynamics of water molecules in the first hydration layer around the thymine NH and adenine NH_2 groups. Instead, fluctuating forces originating from the DNA oligomers and their counterions are considered the main mechanism of the subpicosecond NH stretch dephasing. OH stretching excitations in the water shell around fully hydrated DNA show spectral diffusion on a time scale of 500 fs, substantially slower than that in bulk water. The center line slopes of the 2D spectra of hydrated DNA reveal a strongly reduced amplitude of the initial fast sub-100 fs decay and a slowing down of the correlation decay between 100 and 500 fs when compared with 2D data for neat water and with the calculated frequency−time correlation function. This behavior is attributed to a strongly reduced rate of resonant vibrational energy transfer and the suppression of low-frequency motions in the first water shell around DNA. The observed limited slowing down of the water response compared to bulk water is in line with molecular dynamics simulations of DNA hydration but rules out a slowing down by orders of magnitude in time.

■ ASSOCIATED CONTENT

Supporting Information. 2D spectra of DNA oligomers at a hydration level of 33% RH and the formation of a vibrationally hot ground state of the water shell. This material is available free of charge via the Internet at http://pubs.acs.org.

■ AUTHOR INFORMATION

Corresponding Author

*Phone: +49 30 63921400. Fax: +49 30 63921409. E-mail: elsasser@mbi-berlin.de.

■ ACKNOWLEDGMENT

The research leading to these results has received funding from the European Research Council under the European Union's Seventh Framework Programme (FP7/2007-2013)/ERC Grant Agreement N° 247051. We would like to thank Erik T. J. Nibbering, Henk Fidder (MBI), Damien Laage, ENS Paris, and Casey Hynes, University of Colorado, Boulder, for valuable discussion.

■ REFERENCES

(1) Saenger, W. *Principles of Nucleic Acid Structure*; Springer: New York, 1984.
(2) Edelhoch, H.; Osborne, J. C. *Adv. Protein Chem.* **1976**, *30*, 183–245.
(3) Nibbering, E. T. J.; Elsaesser, T. *Chem. Rev.* **2004**, *104*, 1887–1914.
(4) Laage, D.; Hynes, J. T. *Science* **2006**, *311*, 832–835.
(5) Bakker, H. J.; Skinner, J. L. *Chem. Rev.* **2010**, *110*, 1498–1517.
(6) Drew, H. R.; Dickerson, R. E. *J. Mol. Biol.* **1981**, *151*, 535–556.
(7) Kopka, M. L.; Fratini, A. V.; Drew, H. R.; Dickerson, R. E. *J. Mol. Biol.* **1983**, *163*, 129–146.
(8) Schneider, B.; Cohen, D. M.; Schleifer, L.; Srinivasan, A. R.; Olson, W. K.; Berman, H. M. *Biophys. J.* **1993**, *65*, 2291–2303.
(9) Schneider, B.; Berman, H. M. *Biophys. J.* **1995**, *69*, 2661–2669.
(10) Schneider, B.; Patel, K.; Berman, H. M. *Biophys. J.* **1998**, *75*, 2422–2434.
(11) Saenger, W.; Hunter, W. N.; Kennard, O. *Nature* **1986**, *324*, 385–388.

(12) Forsyth, V. T.; Mahendrasingam, A.; Pigram, W. J.; Greenall, R. J.; Bellamy, K.; Fuller, W.; Mason, S. A. *Int. J. Biol. Macromol.* **1989**, *11*, 236–240.
(13) Tsuboi, M. *J. Am. Chem. Soc.* **1957**, *79*, 1351–1354.
(14) Falk, M.; Hartman, K. A.; Lord, R. C. *J. Am. Chem. Soc.* **1962**, *84*, 3843–3846.
(15) Falk, M.; Hartman, K. A.; Lord, R. C. *J. Am. Chem. Soc.* **1963**, *85*, 387–391.
(16) Liepinsh, E.; Otting, G.; Wuthrich, K. *Nucl. Acid Res.* **1992**, *20*, 6549–6553.
(17) Halle, B.; Denisov, V. P. *Biopolymers* **1998**, *48*, 210–233.
(18) Phan, A. T.; Leroy, J. L.; Guéron, M. *J. Mol. Biol.* **1999**, *286*, 505–519.
(19) Schreiner, L. J.; MacTavish, J. C.; Rupprecht, A. *Biophys. J.* **1991**, *59*, 221–234.
(20) Beveridge, D. L.; McConnell, K. J. *Curr. Opin. Struct. Biol.* **2000**, *10*, 182–196.
(21) Pettitt, B. M.; Makarov, V. A.; Andrews, B. K. *Curr. Opin. Struct. Biol.* **1998**, *8*, 218–221.
(22) Feig, M.; Pettitt, B. M. *J. Mol. Biol.* **1999**, *286*, 1075–1095.
(23) Bonvin, A. M. J. J.; Sunnerhagen, M.; Otting, G.; van Gunsteren, W. F. *J. Mol. Biol.* **1998**, *282*, 859–873.
(24) Pal, S.; Maiti, P. K.; Bagchi, B. *J. Chem. Phys.* **2006**, *125*, 234903.
(25) Pal, S. K.; Zhao, L.; Zewail, A. H. *Proc. Natl. Acad. Sci. U.S.A.* **2003**, *100*, 8113–8118.
(26) Andreatta, D.; Lustres, L. P.; Kovalenko, S. A.; Ernsting, N. P.; Murphy, C. J.; Coleman, R. S.; Berg, M. A. *J. Am. Chem. Soc.* **2005**, *127*, 7270–7271.
(27) Zhong, D.; Pal, S. K.; Zewail, A. H. *Chem. Phys. Lett.* **2011**, *503*, 1–11.
(28) Halle, B.; Nilsson, L. *J. Phys. Chem. B* **2009**, *113*, 8210–8213.
(29) Furse, K. E.; Corcelli, S. A. *J. Am. Chem. Soc.* **2008**, *130*, 13103–13109.
(30) Furse, K. E.; Corcelli, S. A. *J. Phys. Chem. B* **2010**, 9934–9945.
(31) Hamm, P.; Zanni, M.; *Concepts and Methods of 2D Infrared Spectroscopy*; Cambridge University Press: Cambridge, U.K., 2011.
(32) Asplund, M. C.; Zanni, M. T.; Hochstrasser, R. M. *Proc. Natl. Acad. Sci. U.S.A.* **2000**, *97*, 8219–8224.
(33) Mukamel, S. *Annu. Rev. Phys. Chem.* **2000**, *51*, 691–729.
(34) Cowan, M. L.; Bruner, B. D.; Huse, N.; Dwyer, J. R.; Chugh, B.; Nibbering, E. T. J.; Elsaesser, T.; Miller, R. J. D. *Nature* **2005**, *434*, 199–202.
(35) Asbury, J. B.; Steinel, T.; Kwak, K.; Lawrence, C. P.; Skinner, J. L.; Fayer, M. D. *J. Chem. Phys.* **2004**, *121*, 12431–12446.
(36) Krummel, A. T.; Zanni, M. T. *J. Phys. Chem. B* **2006**, *110*, 13991–14000.
(37) Yang, M.; Szyc, Ł.; Elsaesser, T. *J. Phys. Chem. B* **2011**, *115*, 1262–1267.
(38) Dwyer, J. R; Szyc, Ł.; Nibbering, E. T. J.; Elsaesser, T. *J. Phys. Chem. B* **2008**, *112*, 11194–11997.
(39) Szyc, Ł.; Dwyer, J. R.; Nibbering, E. T. J.; Elsaesser, T. *Chem. Phys.* **2009**, *357*, 36–44.
(40) Szyc, Ł.; Yang, M.; Elsaesser, T. *J. Phys. Chem. B* **2010**, *114*, 7951–7957.
(41) Tanaka, K.; Okahata, Y. *J. Am. Chem. Soc.* **1996**, *118*, 10679–10683.
(42) Yang, C.; Moses, D.; Heeger, A. J. *Adv. Mater.* **2003**, *15*, 1364.
(43) Leslie, A. G. W.; Arnott, S.; Chandrasekaran, R.; Ratcliff, R. L. *J. Mol. Biol.* **1980**, *143*, 49–72.
(44) Lipanov, A. A.; Beglov, D. B.; Chuprina, V. B. *J. Mol. Biol.* **1989**, *210*, 399–409.
(45) Mazur, A. K. *J. Chem. Theory Comput.* **2005**, *1*, 325–336.
(46) Taillandier, E.; Liquier, J.; Taboury, J. A. In *Advances in Infrared and Raman Spectroscopy*; Clark, R. J. H., Hester, R., Eds.; John Wiley and Sons: New York, 1985; pp 65−115.
(47) Pilet, J.; Brahms, J. *Biopolymers* **1973**, *12*, 387–403.
(48) Kraemer, D.; Cowan, M. L.; Paarmann, A.; Huse, N.; Nibbering, E. T. J.; Elsaesser, T.; Miller, R. J. D. *Proc. Natl. Acad. Sci. U.S.A.* **2008**, *105*, 437–442.
(49) Cowan, M. L.; Ogilvie, J. P.; Miller, R. J. D. *Chem. Phys. Lett.* **2004**, *386*, 184–189.
(50) Khalil, M; Demirdöven, N.; Tokmakoff, A. *J. Phys. Chem. A* **2003**, *107*, 5258–5279.
(51) Kwak, K.; Park, S.; Finkelstein, I. J.; Fayer, M. D. *J. Chem. Phys.* **2007**, *127*, 124503.
(52) Urabe, H.; Hayashi, H.; Tominaga, Y.; Nishimura, Y.; Kubota, K.; Tsuboi, M. *J. Chem. Phys.* **1985**, *82*, 531–535.
(53) Cocco, S.; Monasson, R. *J. Chem. Phys.* **2000**, *112*, 10017–10033.
(54) Perepelytsya, S. M.; Volkov, S. N. *Eur. Phys. J. E* **2007**, *24*, 261–269.
(55) Prescott, B.; Steinmetz, W.; Thomas, G. J., Jr. *Biopolymers* **1984**, *23*, 235–256.
(56) Jansen, T. I. C.; Auer, B. M.; Yang, M.; Skinner, J. L. *J. Chem. Phys.* **2010**, *132*, 224503.
(57) Paarmann, A.; Hayashi, T.; Mukamel, S.; Miller, R. J. D. *J. Chem. Phys.* **2008**, *128*, 191103.
(58) Woutersen, S.; Bakker, H. J. *Nature* **1999**, *402*, 507–509.